

CrystEngComm

Accepted Manuscript



This is an *Accepted Manuscript*, which has been through the Royal Society of Chemistry peer review process and has been accepted for publication.

Accepted Manuscripts are published online shortly after acceptance, before technical editing, formatting and proof reading. Using this free service, authors can make their results available to the community, in citable form, before we publish the edited article. We will replace this *Accepted Manuscript* with the edited and formatted *Advance Article* as soon as it is available.

You can find more information about *Accepted Manuscripts* in the [Information for Authors](#).

Please note that technical editing may introduce minor changes to the text and/or graphics, which may alter content. The journal's standard [Terms & Conditions](#) and the [Ethical guidelines](#) still apply. In no event shall the Royal Society of Chemistry be held responsible for any errors or omissions in this *Accepted Manuscript* or any consequences arising from the use of any information it contains.

Cite this: DOI: 10.1039/c0xx00000x

www.rsc.org/xxxxxx

Paper

Bottom-Up Synthesis of Cerium-Citric Acid Coordination Polymers Hollow Microspheres with Tunable Shell Thickness and Their Corresponding Porous CeO₂ Hollow Spheres for Pt-Based Electrocatalyst

Zhurui Shen^a, Ji Liu^b, Fangyun Hu^b, Song Liu^a, Ning Cao^a, Ying Sui^a, Qingdao Zeng^{*b}, Yongtao Shen^{*a}

Received (in XXX, XXX) Xth XXXXXXXXX 20XX, Accepted Xth XXXXXXXXX 20XX

DOI: 10.1039/b000000x

Dispersed cerium based CPs hollow microspheres derived from the “green” ligand-citric acid were fabricated for the first time via a bottom-up and template-free way under hydrothermal condition. The shell thickness of hollow spheres could be facially tuned by changing the reaction time, and the morphology could also be regulated by tuning the pH values and molar ratios of reactants. The formation mechanism of hollow microspheres was demonstrated as an Ostwald ripening process, and the release of H₂Cit⁻ was proposed as the promotion of the hollowing process. Moreover, with the CPs hollow spheres as precursors, corresponding porous CeO₂ hollow spheres were obtained, and after loading with Pt, the Pt/CeO₂ electrodes displayed a relative high current density and I_p/I_b value for electrocatalysis of methanol.

Introduction

Coordination polymers (CPs) or metal organic frameworks (MOF) have been widely applied in catalysis, nonlinear optics, gas storage and medicine because of their diverse topological structures and compositions.¹⁻⁵ Currently, the morphogenesis of CPs micro- and nanostructures including the amorphous “infinite coordination polymer” and the crystalline ones have attracted great attention due to their unique and highly tailorable properties.⁶⁻²¹ And for the past few years, kinds of CPs micro- or nanostructures have been synthesized, such as micro- nanospheres,⁶⁻⁹ nanoparticles,¹⁰ nanocubes,^{11,14} nanorods,^{16,17} nanotubes,¹⁸ macroporous foams¹⁹ and nanoflakes.²⁰ These micro- or nano- materials have shown diverse functionalities, including optical properties,⁹ ion exchange,¹¹ magnetism¹⁸ and electrical properties²¹ etc. Moreover, these examples also prove that the size, shape, and composition of CPs are crucial for deciding their chemical and physical properties. Although remarkable progresses have been made in this field, it is still a challenge to design CPs with a certain morphology and function based on a given set of metal cations and ligands.

Hollow structures, especially the hollow spheres have drawn considerable interest in the past few decades due to their low density, large surface area, and wide range of potential applications.²²⁻²⁶ For instance, the large fraction of void space in hollow structures can be used to load and control releasing of drugs, genes, peptides and other biological molecules.²³ They can also be used to modulate refractive index, lower density, increase the active area for catalysis or adsorption and improve particles'

ability to suppress cyclic changes in volume for lithium batteries.²⁴⁻²⁶ Similar effects can be expected in CPs hollow structures, and in some certain conditions, might have better exhibition, for example, in drug delivery due to their lower toxicity.²⁷ However, there are relative few efforts have thus been made towards the successful preparation of CPs hollow spheres.²⁸⁻³² Chen and his coworkers have reported a template free fabrication of lanthanide-asparagine CPs hollow spheres in an early stage.²⁸ Then, Wang et al. have prepared well defined hollow iron- and cobalt-based ferrocenyl coordination polymer microspheres (Fe-Fc-HCPS) with microporous shells by a solvothermal reaction.^{29,30} Recently, Zhong et al. have synthesized series of terbium based hollow spheres with submicrometer size, and these spheres showed an interesting white light emission property.³¹ Although the research for hollow spheres with other compositions have proved that dispersed morphology and tunable shell thickness were very important for their applications,²² reports on effective control of these two factors for hollow CPs spheres are very limited.³² As a result, some new examples and methods are still desired for obtaining CPs hollow spheres with dispersed morphology and tunable shell thickness.

Citric acid (α -hydroxyl tricarboxylic acid), a kind of low-cost and “green” organic molecules, which could be industrially produced from sustainable resources such as molasses, corns and cassava etc. For a long time, it is well known on account of its important roles in biosystems and physiological processes.³³ Moreover, it was found to be a versatile ligand in coordination chemistry due to its conformational flexibility, its ability to

deprotonate completely or partially, and its diversity in complexing behavior. As a result, many metal–citrate compounds have been structurally characterized.^{33–38} Besides that, citric acids has also been widely used in nanomaterials synthesis to stabilize the nuclei, regulate the morphology or act as an important surface exchange ligands due to its strong complex ability with metal cations.^{39–41} Although citric acids has played important roles in coordination chemistry and nanoscience, there are still very few report focusing on its own nanomaterials when complexing with metal cations to form an infinite coordination polymers.

In this regard, we present a bottom-up approach for obtaining cerium-citric acid CPs (denoted as CeCit) hollow microspheres with dispersed morphology by a one-pot hydrothermal reaction without any additional template, and their shell thickness could be facially tuned by varying reaction time. The formation mechanism of hollow spheres was discussed and it can be ascribed to Ostwald ripening. Furthermore, using these CeCit CPs microspheres as precursors, well defined CeO₂ hollow spheres were obtained by calcination. Recently, several kinds of uniform CeO₂ hollow spheres have been fabricated via the template free way, but their methods showed difference with ours. Some of them used the oxidants to fabricate CeO₂ nanopartilces, and then assembled these nanoparticles into hollow spheres using organic reagents such as citric acid⁴², PEG⁴³ and PVP⁴⁴ as the capping agents or structure directing agents, respectively. While others prepared CeO₂ hollow structures through the inorganic intermediates such as Ce(OH)CO₃.^{45,46} However, in our method, the citric acid was not the capping agents or structure directing agents like those in the above literatures, but actually the ligands in the CeCit CPs, and the sperical morphology derived from the initial formed CPs microspheres similar with other amorphous CPs spheres.^{6,7,9} After loading with platinum (Pt), the as-prepared Pt/CeO₂ electrodes displayed a relative high current density and I_F/I_b value for methanol electro-catalysis. Our work offered a simple method to obtain the CPs hollow structures, and the low-cost, enviromental benign citric acid ligands would be beneficial for its conversion to oxides and possible mass production in future.

Experimental section

Materials: All chemical reagents are commercially available and were used as received. Ce(NO₃)₃·6H₂O, citric acids (H₃Cit), concentrated HCl solution (37%) and NaOH were purchased from Guangfu Ltd..

Preparation of Ce-Cit CPs hollow microspheres: In a typical synthesis, 6 mmol H₃Cit was dissolved in 24 ml H₂O. Then 2 mmol Ce(NO₃)₃·6H₂O was added in the H₃Cit solution under stirring. After stirring for several minutes, the solution obtained was transferred into 30 mL autoclave, sealed and heated under 160 °C for certain time. The pH values were tuned using 1M HCl and 1M NaOH, and the quantity of reactants was also tuned if necessary. The as-prepared CeCit CPs was washed by H₂O and ethanol successively and dried at 60 °C.

Preparation of CeO₂ hollow spheres: Using the CeCit CPs hollow spheres as precursors, after calcination at 365 °C for 1.5 h, CeO₂ hollow spheres were obtained.

Preparation of electrocatalyst: Pt/CeO₂ catalyst was prepared in the following steps. 10 mg CeO₂ was dispersed in deionized water

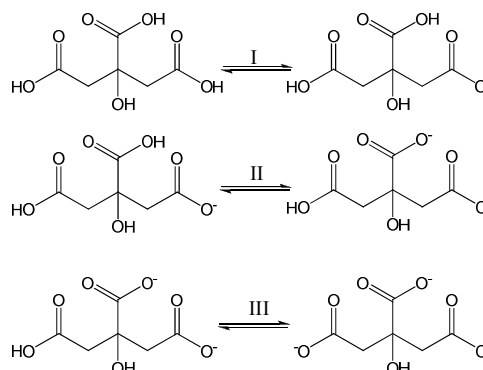
to reach a concentration of 1mg. mL⁻¹, and then mixed with H₂PtCl₄ solution (1 wt%) to make certain quantity of H₂PtCl₄ transferred onto the CeO₂ (here the quantity is 20wt % Pt) under stirring for 1h. After that, H₂PtCl₄ was reduced to metal Pt with the addition of NaBH₄ (5 wt%) under stirring for another 1 h. Before testing, the Pt/CeO₂ particles were mixed with the required amount (20 wt% compared with catalyst) of carbon black (Vulcan XC-72R) in ethanol (total 2.5 mg catalyst and 0.5mg carbon in 5 mL) and placed in ultrasonic treatment for 20 min. After that, 10 μL of suspension was dropped on a glassy carbon electrode and dried at room temperature under nitrogen as protection.

Evaluation of electrocatalyst: All electrochemical measurements were performed on a CHI 650D electrochemical workstation (Shanghai CH Instruments Co.,China). A conventional three-electrode system was used for all electrochemical measurements: a glassy carbon electrode (GC, 0.2 cm²) as the working electrode, an Ag/AgCl electrode as the reference electrode, and a platinum wire electrode as the counter electrode.

Characterization: SEM was measured on Shimadzu SS-550, Hitachi Model S-4800 and Nova instruments. TEM was measured by Philips Tecnai F20 instruments. EDX spectrum was measured on the Hitachi Model S-4800 instrument. The TG-DTA of the sample was performed on a Rigaku TG-DTA thermal analyzer. XRD patterns were recorded on a Rigaku D/max-2500 diffractometer, with Cu Kα radiation at 40 kV and 100 mA. FT-IR spectra were carried out on KBr pellets on a BRUKER VECTOR 22 spectrometer. ¹³C CP/MAS NMR were measured on the Bruker Avance III 400MHz NMR spectrometer. The ESI-MS was performed on Agilent LC (1260)-MS (6520) spectrometer and Bruker Daltonics Apex II FT-ICR-MS Multi-Source Mass Spectrometer System. Element analysis data were obtained with an Elementar Vario-EL instrument. N₂ adsorption and desorption isotherms were measured on a BELSORP miniII analyzer at 77 K. Specific surface area of CeO₂ hollow spheres was calculated by BET (Brunauer-Emmett-Teller) method.

Results and discussion

In a typical synthesis, 6 mmol citric acid (H₃Cit) was employed together with 2 mmol cerium cations (Ce³⁺) to fabricate CeCit CPs hollow spheres under 160 °C in an aqueous solution (Scheme S1). The reaction time, pH value and molar ratio of reactants were all important factors in the formation and regulation of CeCit CPs hollow spheres.



Scheme 1 Illustration of three level ionization of citric acid in aqueous solution.

The morphology of as-prepared CeCit CPs was studied by scanning electron microscopy (SEM) measurements. As shown in Figure 1a, most of the CeCit CPs obtained after reaction for 12 h (denoted as CeCit-12) were hollow microspheres with the diameter of 4-6 μm (CeCit-12: 5.1 μm in average, Figure S 1a; CeCit-24: 5.5 μm in average, Figure S1b). The enlarged picture (Figure 1b, Figure S2a,c) displayed that these microspheres had a smooth surface and with the shell thickness of c.a. 400 nm. When the reaction time was prolonged to 24 h, the as-prepared products (denoted as CeCit-24) were also microspheres with the similar diameter but much better dispersity (Figure 1c), and their enlarged pictures showed that the surface of this patch of microspheres was rougher than that of the ones obtained after shorter reaction time (Figure 1d). Moreover, after another 12 h of reaction, the shell thickness of hollow spheres were obviously decreased (Figure 1d), and its value of a single broken microsphere was measured to be c.a. 150 nm (Figure S2b,d), which is nearly 40% of the ones obtained after reaction of 12h. This phenomenon might be induced by a mass transfer process described below, and could be used to get continuous changed shell thickness by finely tuning the reaction time.

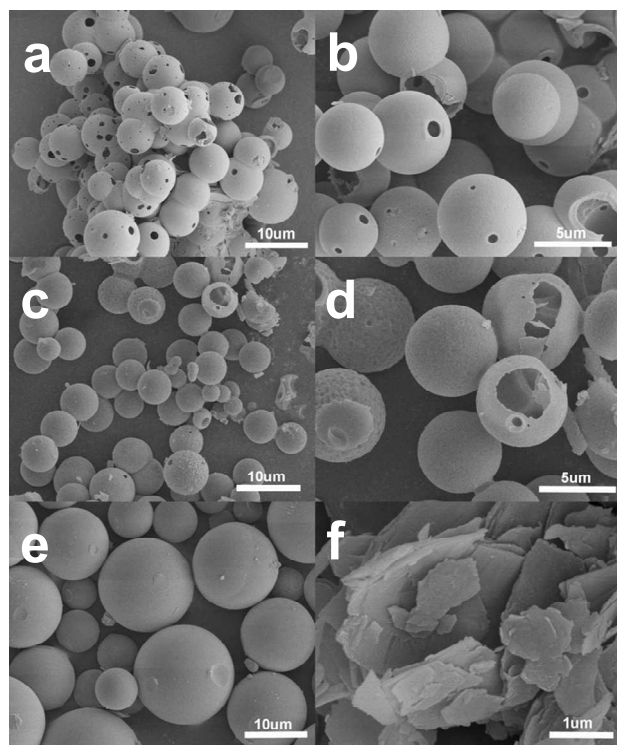
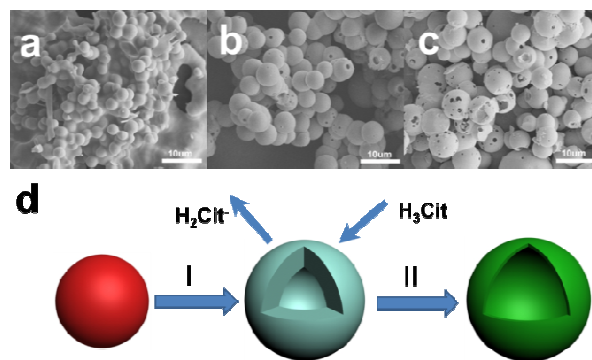


Fig. 1 SEM images of CeCit CPs hollow microspheres obtained after hydrothermal reaction of (a, b) 12 h with pH=2.0, (c, d) 24 h with pH=2.0, (e) 12 h with pH=1.0 and (f) 12 h with pH=3.5.

Another interesting phenomenon is the pH sensitivity of the morphology. The hollow microspheres could only be produced at the pH value of 2.0, while the pH value was tuned below 1.0; microspheres with concrete interiors were obtained (Figure 1e). When the pH value changed to 3.5, microplates with thickness less than 100 nm rather than spherical particles became the main products (Figure 1f), and after tuning the pH value larger than 6,

no solid product was collected. The reason might be ascribed to different ligands formed at varied pH values. The H_3Cit is a kind of weak acid which has three level of ionization ($\text{pK}_{\text{a}1}$ of $\text{H}_3\text{Cit} = 3.13$, $\text{pK}_{\text{a}2} = 4.76$, $\text{pK}_{\text{a}3} = 6.40$, Scheme 1). When the pH value was below 1.0, most of the citric acids existed in the solution as H_3Cit without ionization. So the ligands coordinated with Ce^{3+} were mainly H_3Cit , and the solid microspheres were obtained at that pH value. When the pH value was 3.5, H_2Cit^- rather than H_3Cit dominated the ligands, so microplates instead of microspheres were the main products. While at the pH value of 2.0, the ligands were mixtures of H_3Cit and H_2Cit^- , which might make the CPs in a metastable stage between solid spheres and microplates, so the final products were hollow spheres. Once the pH value increased above 6.0, the H_3Cit approach fully ionization and most ligands were Cit^{3-} . It has stronger solvation ability than H_2Cit^- and HCit^{2-} and could not form stable complexes or CPs with Ce^{3+} , which might be the reason for no solid product. By electrospray ionization mass spectrometry (ESI-MS), fractional ions of $[(\text{C}_6\text{H}_8\text{O}_7)\text{-H}]^-$ ($m/z=191$) were detected for all these three kinds of CPs but no other fragments assigned to HCit^{2-} or Cit^{3-} could be found, which proved the ligands were mainly the mixtures of H_3Cit and H_2Cit^- in the range of pH=1.0~3.5. The morphology could also be facily tuned by molar ratios of reactants, the quantity of H_3Cit was kept unchanged and irregular nanoparticles were obtained at Ce^{3+} quantity of 0.5, 4, 6 and 8 mmol, respectively (Figure S3).

The X-ray diffraction (XRD) patterns of CeCit CPs hollow microspheres were featureless, indicating the non-crystalline or amorphous nature of these materials (Figure S4). As most of reported CPs micro or nano-particles displayed unexplored crystalline structures, and the single crystal could hardly be obtained, researchers usually used multi-analysis methods to study the compositions and structures of CPs micro or nano-particles.^{17,19} Here as an example, the CeCit-12 obtained was carefully characterized.



I: aggregation and hollowing II: continuous hollowing

Fig. 2 SEM images of CeCit CPs obtained after hydrothermal reaction of (a) 2 h, (b) 6 h and (c) 12 h; (d) the illustration of formation process of CeCit CPs hollow microspheres.

Compared with pure citric acid (H_3Cit) ligands, the fourier transform infrared (FT-IR) spectrum (Figure S5a, b) of CeCit-12 CPs displayed similar characteristic except several bands. The strong stretching band at 1620 cm^{-1} and 1690 cm^{-1} in the spectrum of pure H_3Cit could be ascribed to the symmetric and

asymmetric stretching of $-\text{COOH}$. For CPs, these two bands became broader and overlapped with each other due to the coordination effect of Ce^{3+} and carboxyl.^{19,28} The strong bands in 1400 cm^{-1} for H_3Cit and 1410 cm^{-1} for CPs could be assigned to $-\text{CH}_2$ group deformation, which indicated that the bone of ligands was stable during the hydrothermal reaction. In the region of $3600\text{--}3200\text{ cm}^{-1}$, for H_3Cit , there was a strong band centred at 3400 cm^{-1} assigned to $-\text{OH}$ groups. While for CPs, this band was much broader due to the coordination effect. The ^{13}C -nuclear magnetic resonance (NMR) spectrum of CeCit CPs (Figure S6) showed a wide and overlapped spectrum due to the paramagnetic property of cerium and the coordination effect of metal cations and ligands.¹⁹ However, it still displayed the main characteristic of citric acid species including the signal at c.a. 40 ppm of $-\text{CH}_2$ only connected with carboxyl, the signal at c.a. 80 ppm of quaternary carbon connected with both hydroxyl as well as carboxyl and the signal at c.a. 180 ppm of carboxyl groups, which further proved the existence of citric acids species in the CeCit-12 CPs.

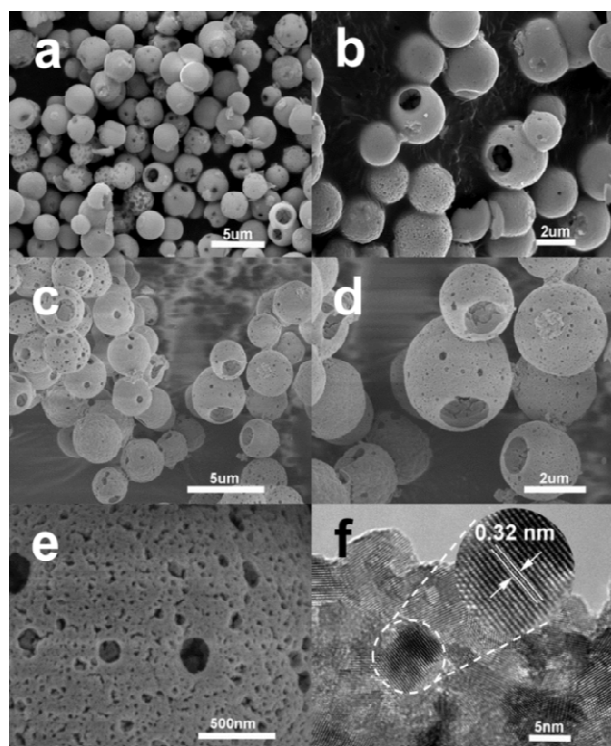


Fig. 3 SEM images of CeO_2 hollow spheres (a, b) CeO_2 -12, (c, d, e) CeO_2 -24; (f) HRTEM image of CeO_2 -24, the inset of the image indicated the crystalline lattices of CeO_2 . These CeO_2 hollow spheres were all prepared by calcination of CeCit CPs precursors obtained at $\text{pH}=2.0$.

By ESI-MS we detected several kinds of molecular fragments of CeCit-12 CPs (Table S1), including $m/z=190.9$ ($[(\text{C}_6\text{H}_8\text{O}_7)\text{-H}]^-$), $m/z=712.0$ ($[\text{Ce}(\text{C}_6\text{H}_8\text{O}_7)_3\text{-4H}]^-$), $m/z=780.9$ ($[\text{Ce}_3(\text{C}_6\text{H}_8\text{O}_7)_6\text{-11H}]^{2-}$) and $m/z=849.1$ ($[\text{Ce}_4(\text{C}_6\text{H}_8\text{O}_7)_6\text{-14H}]^{2-}$), respectively, which provided direct evidence that the infinite coordination network was mainly formed by coordination of Ce^{3+} and citric acid species. Although no obvious molecular fragments of single HCit^{2-} or Cit^{3-} were detected by ESI-MS, we could not fully exclude the involving of these ligands in the CeCit CPs due to their possible existence by deprotonating of H_3Cit (or H_2Cit^-) and

coordinating with Ce^{3+} . Based on the above analysis, Elemental analysis (EA) data (Table S2) and weight loss information of thermogravimetry (TGA) (Figure S7), the chemical composition of the CeCit-12 could be derived as $\text{Ce}_{0.89}(\text{C}_6\text{H}_{5.33}\text{O}_7) \cdot 1.54\text{H}_2\text{O}$. $\text{C}_6\text{H}_{5.33}\text{O}_7$ was the average composition of mixed citric acids species, which might also be one reason for the formation of amorphous CPs.

To elucidate the formation mechanism of CeCit hollow microspheres, as an example, the CeCit-12 was carefully studied here. The time-dependent syntheses were performed at $160\text{ }^\circ\text{C}$ and the products obtained at different reaction times were subjected to SEM, XRD, FT-IR and EA measurements, respectively. It is interesting to note that, after 2 h of reaction, most of the initial products were microspheres of size c. a. $1\text{--}3\text{ }\mu\text{m}$, and some of them started to aggregate into larger ones (Figure 2a). After 6 h of reaction, microspheres with diameter of $4\text{--}6\text{ }\mu\text{m}$ were mainly produced, and partial microspheres began to hollow out (Figure 2b). After the reaction proceeded to 12 h, the final hollow microspheres were prepared (Figure 2c). The XRD patterns showed that the CPs obtained at 6 h and 12 h were all in amorphous nature (Figure S4b,c), while the pattern of initial products (2 h) had a rough baseline similar to other CPs but with several weak peaks (Figure S4a). The FT-IR spectra of CPs obtained in the initial stage (Figure S5c, d) showed the similar characteristics to those of pure H_3Cit and CeCit-12, indicating the preservation of citric acids in the CPs. However, they displayed different subtle structures especially in the region of $1800\text{--}1200\text{ cm}^{-1}$ compared with CeCit-12, which was consistent with the XRD patterns and proved again the different nature between the poor crystallized CPs in the initial stage (2 and 6 h) and the amorphous CPs obtained after reaction exceeding 12h.

It is known that the citric acids existed in the initial reaction solution were almost the mixtures of H_3Cit and H_2Cit^- ($\text{pH}=2.0$), and the crystalline microplates (Figure 1f) obtained at $\text{pH}=3.5$ mainly contained H_2Cit^- . So it is suggested that the ligands in the initial products were probably the mixture of H_3Cit and H_2Cit^- , and the CPs containing mixed ligands could be recognized as a metastable stage between solid microspheres (H_3Cit as ligands) and crystalline microplates (H_2Cit^- as ligands). As a result, when the hydrothermal reaction proceeded, the H_2Cit^- were gradually released and the crystalline phase in the initial product decomposed, which resulted in the formation of void in microspheres (Figure 2a-c) and disappearance of crystalline peaks in XRD pattern (Figure S4). The mass release was also proved by EA analysis (Table S2), which showed that the content of carbon in products gradually decreased during the reaction process. Notably, the total decreasing of carbon quantity (from 2 h to 12 h) was 1.48 wt%, which is not enough compared to the large void in the hollow microspheres. That is because the quantity of citric acids is much excessive, and the outcome of H_2Cit^- was together with income of H_3Cit during the reaction process, which might bring enough Ce- H_3Cit phase to stabilize the final product and was proved by a slightly increasing of hydrogen (Table S2). Due to the excess of H_3Cit ligands, some free H_3Cit molecules could also be encapsulated in the shells of CPs during this process. Zeng have suggested that Ostwald ripening could also be operative for amorphous solids,⁴⁷ and in our previous work, both of the particles aggregation and hollowing process of amorphous CPs

were proved to follow Ostwald ripening mechanism, and the driving forces were release of organic ligands.^{19,28} So combined the results described above, it is demonstrated that the hollow microspheres were probably formed by a particle aggregation together with hollowing process based on Ostwald ripening mechanism, and the promotion is the release of H_2Cit^- (Figure 2d).

Recently, conversions of CPs into nanostructured metal oxides or carbon materials have become an important application of CPs due to their diversity and adjustability in morphology and compositions.^{19,20,28,48-51} Besides that, CeO_2 is a kind of excellent inorganic materials which have wide applications in catalysis, biology, ionic conductor and solid oxides fuel cells etc.⁵²⁻⁵⁵ As a result, here with CeCit CPs hollow spheres as precursors, dispersed CeO_2 hollow spheres with porous shell were obtained by calcination (Figure 3, Figure S7 and Figure S8).

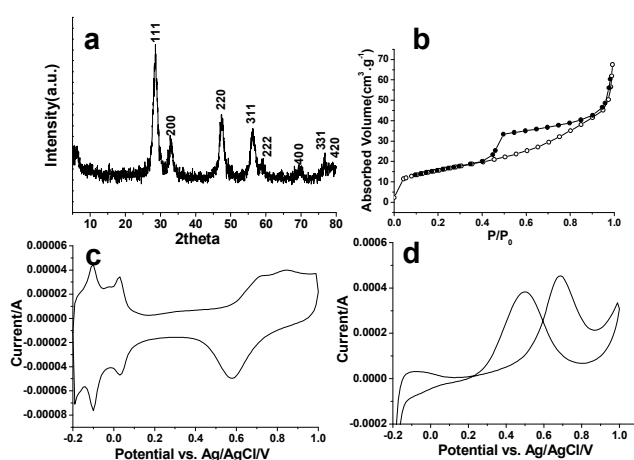


Fig. 4 (a) The XRD pattern and (b) the nitrogen adsorption and desorption isotherms of CeO_2 -24; the cyclic voltammograms of Pt/ CeO_2 -24 (20% wt Pt) in (c) 0.5 M H_2SO_4 and in (d) 0.5 M H_2SO_4 and 1M methanol solution.

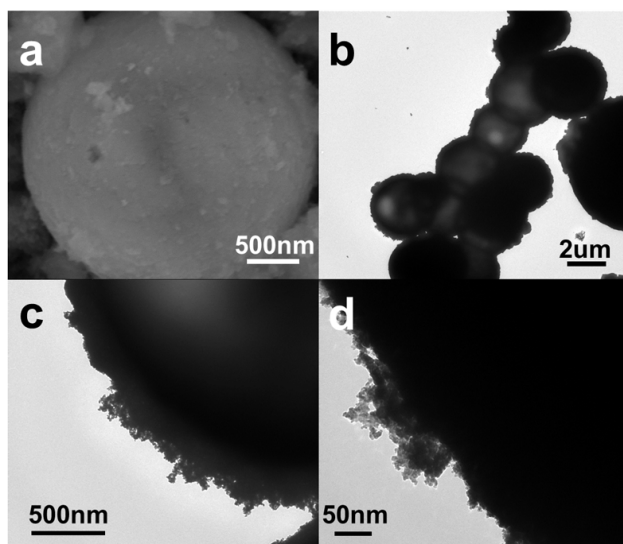


Fig. 5 SEM image (a) and TEM images (b-d) of Pt/ CeO_2 -24.

The SEM images (Figure 3a, c) showed that both of CeO_2 hollow spheres derived from CeCit-12 and CeCit-24 (denoted as CeO_2 -12 and CeO_2 -24, respectively) became shrinkage (about

50%) after calcination, and their diameters were in the range of 2-4 μm (CeO_2 -12, 2.7 μm in average, Figure S1c; CeO_2 -24: 2.5 μm in average, Figure S1d), while their shell thickness did not have obvious change (Figure 3c, d). Another interesting variation after calcination is the increasing of dispersity of these CeO_2 hollow spheres, which might be ascribed to the broken of adhesion parts between spheres (Figure S8a). The magnified images displayed that there were nanopores (20-200 nm) on the shell of CeO_2 hollow spheres (Figure 3b, d, e and Figure S8b), especially for the CeO_2 -24, which should be due to their much thinner shell thickness. So we chose CeO_2 -24 as an example, and studied its porous properties. The broad diffraction peaks in its XRD pattern (Fig 4a) implied that it might be assembled by CeO_2 nanoparticles, and this was confirmed by high resolution transmission electron microscope (HRTEM) test. The HRTEM image (Fig. 3f) showed that the shell of hollow spheres was assembled by CeO_2 nanoparticles with the d-spacing of 0.32 nm. The aggregation of nanoparticles gave rise to a mesoporous structure, with a BET surface area of 56 $\text{m}^2 \cdot \text{g}^{-1}$ (Figure 4b).

CeO_2 has been proved as a kind of effective support or promoter for electrocatalyst after loading noble metals.⁵⁶⁻⁶¹ Here we used CeO_2 -24 as the support and promoter, prepared Pt/ CeO_2 (20 wt% Pt quantity, carbon black was also added to improve the total conductivity) and test its electrocatalytic properties for methanol oxidation. Figure 4c showed the cyclic voltammetry (CV) curve of our Pt/ CeO_2 modified electrodes in 0.5 M H_2SO_4 to evaluate its electrocatalytic activity without the reactants, and it displayed a strong reduction peak at around 0.55 V and an oxidation peak above 0.6 V, which is the characteristic of Pt based materials.⁶²⁻⁶⁵ The existing of these peaks suggested that our Pt/ CeO_2 material had relative strong electrocatalytic activity, so we could perform the reaction in the solution of 1M methanol and 0.5 M H_2SO_4 to evaluate its electrocatalytic activity for methanol oxidation in detail (Figure 4d). The CV curve in methanol showed that there were two oxidation peaks appeared at around 0.4 and 0.65 V with a scanning rate of 50 mV/s. The calculated peak current density was 2.28 $\text{mA} \cdot \text{cm}^{-2}$ (the mass-specified current density of the Pt/ CeO_2 was 91 $\text{mA} \cdot \text{mg}^{-1}$, 0.005 mg catalyst on the glassy carbon electrode), which is no less than other Pt/ CeO_2 modified electrodes with the similar Pt quantity.⁶¹

Ceria promoted noble metal electrocatalysts have been proved to be stable in acidic electrolytes after long time cycling^{59, 60}. Herein, our electrocatalyst also showed stable activity after 200 cycles (Figure S9). One of the possible reasons might be the relative high redox potentials of CeO_2 : from 1.42 V~1.50 V vs. Ag/AgCl in 0.1 M~4 M H_2SO_4 .⁶⁶ Figure 5 showed the microstructure of Pt/ CeO_2 -24. The low resolution TEM image (Figure 5b) displayed several microspheres with pale inner parts further proving their hollow nature. It is observed that although there existed some slight aggregations of Pt nanoparticles, they dispersed relative well to form a layer on the shell of CeO_2 hollow spheres (Figure 4c) with the grain size of about 10 nm (Figure 4d), which might be responsible for its electrocatalytic activity and stability. A typical energy dispersive X-ray (EDX) spectrum was shown in Figure S10, which confirmed the existence of Pt element. Two random quantity of Pt detected by EDX were 14.48 wt% and 27.70 wt%, which were close to the theoretical loading quantity of Pt.

In methanol electro-oxidation, the anodic peak current in the reverse scan (I_b) is for the removal of intermediate CO-like compounds produced during the forward scan (I_f). So the parameter I_f/I_b is very important to evaluate catalyst susceptibility to poisoning.⁶⁷ Low I_f/I_b ratio indicated poor oxidation of methanol to carbon dioxide during the forward scan and excessive accumulation of carbonaceous residues on the catalyst surface, which would lead to catalyst poisoning. While high I_f/I_b ratio indicated better anti-poisoning ability. Here the I_f/I_b value for our Pt/CeO₂ modified electrode is 1.19, which is nearly twice for commercial Pt/C catalyst (0.77)⁶⁷ and indicates the addition of CeO₂ hollow spheres increased the anti-poisoning ability for the whole Pt-based electrodes. Shen et al. demonstrated that during the electrocatalysis, the oxygen containing species could form on the CeO₂ and then transform CO-like poisoning species on Pt to CO₂, leaving the active sites on Pt for further electrochemical reaction.⁵⁶ Recently, Ou and his coworkers have further studied the roles of CeO₂ in Pt/CeO₂ electrodes using HRTEM and electron energy loss spectroscopy (EELS).⁵⁸ They found that the CeO₂ could strongly interact with Pt via a redox process and produce high concentration of defects such as Pt cations, Ce³⁺ cations, and oxygen vacancies in a so-called triple-phase interfacial region (CeO₂-Pt-atmosphere/solution), and these defects could generate and support the OH groups to eliminate the CO like poisoning species on the Pt particles and thus promote the oxidation of methanol. In our case, the relative high I_f/I_b value might be assigned to not only this point but the porous structure as well as high surface area.

Conclusions

In summary, dispersed CeCit CPs hollow microspheres were fabricated here via a bottom-up and template-free way under hydrothermal condition. The shell thickness of hollow spheres could be facially tuned by controlling the reaction time, and the morphology also displayed sensitivity to pH value and molar ratios of reactants. The formation mechanism of hollow microspheres was demonstrated as an Ostwald ripening process, and the release of H₂Cit⁻ was proposed as the promotion of the hollowing process. Moreover, with the CPs hollow spheres as precursors, corresponding porous CeO₂ hollow spheres were obtained, and after loading with Pt, the Pt/CeO₂ electrodes displayed a relative high current density and I_f/I_b value for electrocatalysis of methanol. Our work offered a simple method to obtain the CPs hollow structures, and the low-cost, environmental benign citric acid ligands would be beneficial for its conversion to oxides and possible mass production in future.

Acknowledgements

This work was supported by the Seed Foundation of Tianjin University and the Open Project of Key Lab Adv Energy Mat Chem (Nankai Univ) (KLAEMCOP201201), the National Key Basic Research Program of China (Nos. 2011CB932303, 2013CB934200). And the National Natural Science Foundation of China (Nos. 21073048, 51173031, 21303118, 91127043, 51103094), Key Laboratory of Optoelectronic Materials Chemistry and Physics, Chinese Academy of Sciences (2008DP173016, 2010KL0010) are also gratefully acknowledged.

Notes and references

- ^a Key Laboratory for Advanced Ceramics and Machining Technology of Ministry of Education, Tianjin University & School of material Science and Engineering, Tianjin University, Tianjin 300072, PR China
E-mail: shenyt@tju.edu.cn
- ^b CAS Key Laboratory of Standardization and Measurement for Nanotechnology, National Center for Nanoscience and Technology, 11 Zhongguancun Beiyitiao, Beijing 100190, PR China
E-mail: zenggd@nanoctr.cn
- [†] Electronic Supplementary Information (ESI) available: [SEM, XRD, TGA, IR spectra and ESI-MS results related with CeCit CPs and their corresponding oxides]. See DOI: 10.1039/b000000x/
- M. Brian and M. J. Zaworotko, *Curr. Opin. Solid State Mater. Sci.* 2002, **6**, 7.
 - S. L. James, *Chem. Soc. Rev.* 2003, **32**, 5.
 - J. R. Li, R. J. Kuppler and H.-C. Zhou, *Chem. Soc. Rev.* 2009, **38**, 1477.
 - H. Furukawa, N. Ko, Y. B. Go, N. Aratani, S. B. Choi, E. Choi, A. O. Yazaydin, R. Q. Snurr, M. O'Keeffe, J. Kim and O. M. Yaghi, *Science* 2010, **329**, 424.
 - P. Dechambenoit and J. R. Long, *Chem. Rev. Soc.* 2011, **40**, 3249.
 - M. Oh and C. A. Mirkin, *Nature* 2005, **438**, 651.
 - X. Sun, S. Dong and E. Wang, *J. Am. Chem. Soc.* 2005, **127**, 13102.
 - M. Oh and C. A. Mirkin, *Angew. Chem. Int. Ed.* 2006, **45**, 5492.
 - H. Maeda, M. Hasegawa, T. Hashimoto, T. Kakimoto, S. Nishio and T. Nakanishi, *J. Am. Chem. Soc.* 2006, **128**, 10024.
 - E. Chelebaeva, Y. Guari, J. Larionova, A. Trifonov and C. Guerin, *Chem. Mater.* 2008, **20**, 1367.
 - S. Diring, S. Furukawa, Y. Takashima, T. Tsuruoka and S. Kitagawa, *Chem. Mater.* 2010, **22**, 4531.
 - O. K. Farha, A. M. Spokoyny, K. L. Mulfort, S. Galli, J. T. Hupp, T. Joseph and C. A. Mirkin, *Small*, 2009, **5**, 1727.
 - J. Choi, H. Y. Yang, H. J. Kim and S. U. Son, *Angew. Chem. Int. Ed.* 2010, **49**, 7718.
 - S. Jung and M. Oh, *Angew. Chem. Int. Ed.* 2008, **47**, 2049.
 - Y.-M. Jeon, J. Heo and C. A. Mirkin, *J. Am. Chem. Soc.* 2007, **129**, 7480.
 - W. J. Rieter, K. M. L. Taylor, H. An, W. Lin and W. Lin, *J. Am. Chem. Soc.* 2006, **128**, 9024.
 - K. M. L. Taylor, W. J. Rieter and W. Lin, *J. Am. Chem. Soc.* 2008, **130**, 14358.
 - R. Kaminker, R. Popovitz-Biro and M. E. van der Boom, *Angew. Chem. Int. Ed.* 2011, **50**, 3224.
 - Z. R. Shen, G. J. Zhang, H. J. Zhou, P. J. Sun, B. H. Li, D. T. Ding and T. H. Chen, *Adv. Mater.* 2008, **20**, 984.
 - M. Hu, S. Ishihara and Y. Yamauchi, *Angew. Chem. Int. Ed.* 2013, **52**, 1235.
 - L. Welte, A. Calzolari, R. D. Felice, F. Zamora and J. Gómez-Herrero, *Nat. Nanotechnol.*, 2010, **5**, 110.
 - J. Hu, M. Chen, X. S. Fang and L. M. Wu, *Chem. Soc. Rev.*, 2011, **40**, 5472.
 - Y. Zhu, J. Shi, W. Shen, X. Dong, J. Feng, M. Ruan and Y. Li, *Angew. Chem. Int. Ed.*, 2005, **44**, 5083.
 - J. Yuan, K. Laubernds, Q. Zhang and S. L. Suib, *J. Am. Chem. Soc.*, 2003, **125**, 4966.
 - Y. Zhu, Y. Fang and S. Kaskel, *J. Phys. Chem. C*, 2010, **114**, 16382.
 - Y. Yao, M. T. McDowell, I. Ryu, H. Wu, N. A. Liu, L. B. Hu, W. D. Nix and Y. Cui, *Nano Lett.*, 2011, **11**, 2949.
 - L. Xing, Y. Y. Cao and S. A. Che, *Chem. Commun.* 2012, **48**, 5995.
 - Z. R. Shen, J. G. Wang, P. C. Sun, D. T. Ding and T. H. Chen, *Chem. Commun.* 2009, 1742.
 - J. Huo, L. Wang, E. Irran, H. J. Yu, J. M. Gao, D. S. Fan, B. Li, J. J. Wang, W. B. Ding, A. M. Amin, C. Li and L. Ma, *Angew. Chem. Int. Ed.*, 2010, **49**, 9237.
 - J. Huo, L. Wang, E. Irran, H. J. Yu, L. Ma, J. M. Gao, D. S. Fan, B. Li, J. J. Wang, W. B. Ding, A. M. Amin, C. Li and Y. L. Tai, *J. Colloid. Interf. Sci.*, 2012, **367**, 92.
 - S. L. Zhong, R. Xu, L. F. Zhang, W. G. Qu, G. Q. Gao, X. L. Wu and A. W. Xu, *J. Mater. Chem.* 2011, **21**, 16574.

- 32 J. U. Park, H. J. Lee, W. Cho, C. Jo and M. Oh, *Adv. Mater.*, 2011, **23**, 3161.
- 33 K. E. Wellen, G. Hatzivassiliou, U. M. Sachdeva, T. V. Bui, J. R. Cross and C. B. Thompson, *Science*, 2009, **324**, 1076.
- 34 T. S. Keizer, B. L. Scott, N. N. Sauer and T. M. McCleskey, *Angew. Chem. Int. Ed.* 2005, **44**, 2403.
- 35 I. Gautier-Luneau, C. Merle, D. Phanon, F. Biaso, G. Serratrice and J.-L. Pierre, *Chem. Eur. J.* 2005, **11**, 2207.
- 36 Z. H. Zhou, Y. F. Deng and H. L. Wan, *Cryst. Growth Des.* 2005, **3**, 1109.
- 37 F. Y. Li, L. Xu, G. G. Gao L. H. Fan and B. Bi, *Eur. J. Inorg. Chem.* 2007, 3405.
- 38 J. Lhoste, N. Henry, P. Roussel, T. Loiseau and F. Abraham, *Dalton Trans.*, 2011, **40**, 2422.
- 39 Y. J. Xiong, J. M. McLellan, Y. D. Yin and Y. N. Xia, *Angew. Chem. Int. Ed.* 2007, **46**, 790.
- 40 C. Xue, G. S. Metraux, J. E. Millstone and C. A. Mirkin, *J. Am. Chem. Soc.* 2008, **130**, 8337.
- 41 I. A. Mudunkotuwa and V. H. Grassian, *J. Am. Chem. Soc.* 2010, **132**, 14986.
- 42 J. J. Ma, K. Qian, W. X. Huang, Y. H. Zhu and Q. Yang, *Bull. Chem. Soc. Jpn.* 2010, **83**, 1455.
- 43 L. J. Han, R. J. Liu, C. S. Li, H. H. Li, C. X. Li, G. J. Zhang and J. N. Yao, *J. Mater. Chem.* 2012, **22**, 17079.
- 44 X. F. Liu, H. X. Yang, L. Han, W. Liu, C. Zhang, X. Y. Zhang, S. P. Wang and Y. Z. Yang, *CrystEngComm* 2013, **15**, 7769.
- 45 Z. J. Yang, J. J. Wei, H. X. Yang, L. Liu, H. Liang, and Y. Z. Yang, *Eur. J. Inorg. Chem.* 2010, 3354.
- 46 G. L. Shen, H. D. Liu, Q. Wang, Z. Wang and Y. F. Chen, *J. Nanopart. Res.* 2012, **14**, 954.
- 47 H. C. Zeng, *J. Mater. Chem.* 2006, **16**, 649.
- 48 B. Liu, H. Shioyama, T. Akita and Q. Xu, *J. Am. Chem. Soc.*, 2008, **130**, 5390.
- 49 H. L. Jiang, B. Liu, Y. Q. Lan, K. Kuratani, T. Akita, H. Shioyama, F. Zong and Q. Xu, *J. Am. Chem. Soc.* 2011, **133**, 11854;
- 50 X. Roy, J. K. H. Hui, M. Rabnawaz, G. Liu and M. J. MacLachlan, *Angew. Chem. Int. Ed.* 2011, **50**, 1597.
- 51 M. Hu, J. Reboul, S. Furukawa, N. L. Torad, Q. Ji, P. Srinivasu, K. Ariga, S. Kitagawa and Y. Yamauchi, *J. Am. Chem. Soc.* 2012, **134**, 2864.
- 52 Q. Yuan, H. H. Duan, L. L. Li, Z. X. Li, W. T. Duan, L. S. Zhang, W. G. Song and C. H. Yan, *Adv. Mater.* 2010, **22**, 1475.
- 53 X. H. Guo, C. C. Mao, J. Zhang, J. Huang, W. N. Wang, Y. H. Deng, Y. Y. Wang, Y. Cao, W. X. Huang and S. H. Yu, *Small*, 2012, **8**, 1515.
- 54 C. Menchon, R. Martin, N. Apostolova, V. M. Victor, M. Alvaro, J. R. Herance and H. Garcia, *Small*, 2012, **8**, 1895.
- 55 W. Jung, J. O. Dereux, W. C. Chueh, Y. Hao and S. M. Haile, *Energy Environ. Sci.*, 2012, **5**, 8682.
- 56 C. Xu and Shen, P. K., *Chem. Commun.* 2004, 2238.
- 57 C. W. Xua, Z. Q. Tian, P. K. Shen and S. P. Jiang, *Electrochimica Acta*, 2008, **53**, 2610.
- 58 D. R. Ou, T. Mori, H. Togasaki, M. Takahashi, F. Ye and J. Drennan, *Langmuir* 2011, **27**, 3859.
- 59 K. Kwon, K. H. Lee, S. A. Jin, D. J. You and C. Pak, *Electrochem. Commun.*, 2011, **13**, 1067.
- 60 D. H. Lim, W. D. Lee, D. H. Choi and H. I. Lee, *Appl. Catal. B: Environ.* 2010, **94**, 85.
- 61 Y. Lin, C. Su, C. Huang, J. S. Kim, C. Kwak and Z. P. Shao, *J. Power Sources*, 2012, **197**, 57.
- 62 H. Y. Sun, J. M. You, M. H. Yang and F. L. Qu, *J. Power Sources*, 2012, **205**, 231.
- 63 M. H. Yang, F. L. Qu, Y. S. Lu, Y. He, G. L. Shen and R. Q. Yu, *Biomaterials*, 2006, **27**, 5964.
- 64 R. Wang, C. Wang, W. Cai and Y. Ding, *Adv. Mater.* 2010, **22**, 1845.
- 65 Z. Liu, X. Y. Ling, X. Su and J. Y. Lee, *J. Phys. Chem. B*, 2004, **108**, 8234.
- 66 A. Paulenova, S. E. Creager, J. D. Navratil and Y. Wei, *J. Power Sources*, 2002, **109**, 431.
- 67 Z. W. Chen, M. Waje, W. Z. Li and Y. S. Yan, *Angew. Chem. Int. Ed.*, 2007, **46**, 4060.

The table of contents entry Herein, cerium-citric acid coordination polymers (CPs) hollow microspheres with tunable shell thickness and their corresponding porous CeO₂ hollow spheres for Pt-based electrocatalyst have been reported.

Zhurui Shen, Ji Liu, Fangyun Hu, Song Liu, Ning Cao, Ying Sui, Qingdao Zeng*,
Yongtao Shen*

Cerium-citric acid CPs hollow spheres and the electrocatalytic properties of Pt/CeO₂ hollow spheres

